An informational approach to the Network Disease Hypothesis in resting state fMRI

Jaime Gomez-Ramirez, Yujie Li, Qiong Wu, Xiaoyu Tang, Jinglong Wu

Abstract Network theory approaches to brain connectivity in resting state- fMRI have been mainly focused on the study of topological properties and network motifs that characterize the network structure. The network degeneration hypothesis -disease starts in small network assemblies, to progressively spread to connected areas of the initial locus- has been investigated in a number of brain pathologies. For example, the disruption of normal brain function in diseases such as schizophrenia and Alzheimer's disease can be observed and measured in terms of variations in the network topology. However, a coherent and integrative understanding of the interplay between brain disease and network connectivity is still missing. Here we combine graph and information theory based approaches to understand network robustness in resting state-fMRI. We calculate first how the network robustness is affected upon the removal of any node in the functional connectivity network in resting state for both young and elder subjects. Then, we study the stochastic process defined by a random walk on the functional connectivity graph, to provide information theoretic measures such as the entropy rate of the stationary Markov chain, defined by the transformation of the binary adjacency matrix A into a probability transition matrix T, $T_{ij} = \frac{A_{ij}}{\sum_j A_{ij}}$. We find that the entropy rate of the functional connectivity network modeled as a Markov chain explains why the removal of some nodes increases the efficiency of the informational flow shown in the graph based approach. We argue that the discovery of network based biomarkers for neurodegenerative conditions will rely on the combination of both graph theoretic and informational approaches in Resting-State fMRI

Key words: resting state fMRI, network degeneration hypothesis, Markov chain, relative entropy

---

Biomedical Engineering Laboratory, Okayama University, Japan
Autonomous Systems Laboratory, Universidad Politécnica de Madrid, Spain
e-mail: jd.gomez@upm.es

1 Introduction

It has been suggested that fluctuations in the BOLD signal measured in humans in resting state, represent the neuronal activity baseline and shape spatially consistent patterns [37], [17]. These slow fluctuations in BOLD signal found in resting subjects, are highly coherent within either structural or functional networks in the human brain. Therefore, exploring these fluctuations could lead to a better understanding of the brain's intrinsic or spontaneous neural activity. Functional correlation based on the synchrony of low-frequency blood flow fluctuations in resting state, have been identified in the sensorimotor [24], visual [12], language [21], auditory [22], dorsal and ventral attention [15] and the frontoparietal control system [46]. The systematic study of those patterns using correlation analysis techniques has identified a number of resting state networks, which are functionally relevant networks found in subjects in the absence of either goal directed-task or external stimuli. The visual identification of the overall connectivity patters in resting state functional magnetic resonance imaging (rs-fMRI), has been assessed using either model-based and model-free approaches. In the former, statistical parametric maps of brain activation are built upon voxel-wise analysis location. This approach has been successful in the identification of motor networks, but it shows important limitations when the seed voxel cannot be easily identified. For example, in brain areas with unclear boundaries i.e., cognitive networks involved for instance, in language or memory. Independent Component Analysis (ICA), on the other hand, is a model-free approach that allows separating resting fluctuations from other signal variations, resulting on a collection of spatial maps, one for each independent component, that represent functionally relevant networks in the brain. While ICA has the advantage over model-free methods that it is unbiased, (that is, it does not need to posit a specific temporal model of correlation between ROIs), the functional relevance of the different components is, however, computed relative to their resemblance to a number of networks based on criteria that are not easily formalized. More recently, researchers using graph-theory based methods have been able to not only visualize brain networks, but to quantify their topological properties. Large-scale anatomical connectivity analysis in the mammalian brain, shows that brain topology is neither random nor regular. Instead, small world architectures [49] -highly clustered nodes connected thorough relatively short paths- have been identified in brain networks. Small world networks are not solely structural, functional networks with a small world organization have been identified in the mammal brain [2]. In addition to this, disruptions in the small world organization can give clues about normal development and pathological conditions. For example, Supekar and colleagues [41] have shown that the deterioration of small world properties such as the lowering of the cluster coefficient, affect local network connectivity, which in turn may work as a network biomarker for Alzheimer's disease. Abnormalities in small-worldness may also have a significant positive correlation in, for example, schizophrenia [29] and epilepsy [28]. While network-based studies have been successful in delineating generic network properties, such as path length or clustering, additional work is needed in order to come to grips with the internal working of the systems under-

lying the network. Robustness in brain connectivity has been typically approached in terms of the impact that the complete disruption and/or removal of a network component has in the network topology [23]. However, by focusing on the topology of the network, factors that may play a key role in the network's vulnerability to failures can be neglected. For example, it has been suggested that patients with Alzheimer's disease show an increment in brain activity in certain areas relative to healthy subjects that compensates for the disease related atrophy of other regions [38]. The network degeneration hypothesis, NDH for short, encompasses the idea that neurodegeneration can be studied as a network dysfunction process, in which changes in the network organization are informative about the progression of the disease [40], [34]. The network degeneration hypothesis -disease starts in small network assemblies, to progressively spread to connected areas of the initial locus- has been investigated in a number of brain pathologies including Alzheimer's disease [7], epilepsy [28], schizophrenia [29] and unipolar depression [30]. To our knowledge, the first attempt to systematically test the NDH is in [40], in which Seeley and colleagues use functional and structural network mapping approaches to characterize five distinct neurodegenerative syndromes.

In this paper we explore the network degeneration hypothesis using a methodology that combines graph and information theoretic tools. In section 2 the methodology followed in the data acquisition, data preprocessing, anatomical parcellation and brain network reconstruction in two groups -24 young and 19 elder individuals- is presented. Then we systematically study network robustness -functional network invariance under perturbation- is affected upon the removal of any node in the functional connectivity network in resting state for both young and elder subjects. We provide a ranking of nodes that quantifies the impact of their obliteration using a network efficiency measure based on [25] that quantifies how the network efficiency in transmitting information deteriorates once a node is removed from the network. Next, we study the stochastic process defined by a random walk on the functional connectivity graph, in order to use the entropy rate of the stationary Markov chain, defined by the transformation of the binary adjacency matrix A into a probability transition matrix T, $T_{ij} = \frac{A_{ij}}{\sum_j A_{ij}}$. We find that the entropy rate of the functional connectivity network modeled as a Markov chain explains why the removal of some nodes increases the efficiency of the informational flow shown in the graph based approach.This is explained in the results section 3. the paper clonclude with a discussion section 4 in which it is sketched a new theoretical framework to investigate network robustness and how it is affected by internal perturbations such as aging and neurological disorders.

2 Materials and Methods

2.1 Subjects

Twenty-three healthy male volunteers (ages 21-32; mean 22.7) took part in the fMRI experiment. All subjects had normal or corrected-to-normal vision. The study was approved by the ethics committee of Okayama University, and written informed consent was obtained before the study.

2.2 Data acquisition

All subjects were imaged using a 1.5 T Philips scanner vision whole-body MRI system (Okayama University Hospital, Okayama, Japan), which was equipped with a head coil. Functional MR images were acquired during rest when subjects were instructed to keep their eyes closed and not to think of anything in particular. The imaging area consisted of 32 functional gradient-echo planar imaging (EPI) axial slices (voxel size=3x3x4 mm3, TR=3000 ms, TE=50 ms, FA=90^{o}, 64x64 matrix) that were used to obtain T2*-weighted fMRI images in the axial plane. We obtained 176 functional volumes and excluded the first 4 scans from analysis. Before the EPI scan, a T1-weighted 3D magnetization-prepared rapid acquisition gradient echo (MP-RAGE) sequence was acquired (TR=2300 ms, TE=2.98 ms, TI=900 ms, voxel size=1x1x1 mm3).

2.3 Data preprocessing

Data were preprocessed using Statistical Parametric Mapping software SPM8 [] and REST v1.7 []. To correct for differences in slice acquisition time, all images were synchronized to the middle slice. Subsequently, images were spatially realigned to the first volume due to head motion. None of the subjects had head movements exceeding 2.5 mm on any axis or rotations greater than 2.5^{o}. After the correction, the imaging data were normalized to the Montreal Neurological Institute (MNI) EPI template supplied with SPM8 (resampled to 2x2x2 mm3 voxels) [**?**]. In order to avoid artificially introducing local spatial correlation, the normalized images were not smoothed [**?**]. Finally, the resulting data were temporally band-pass filtered (0.01-0.08 Hz) to reduce the effects of low-frequency drifts and high-frequency physiological noises [**?**].

2.4 Anatomical parcellation

Before whole brain parcellation, several sources of spurious variance including the estimated head motion parameters, the global brain signal and the average time series in the cerebrospinal fluid and white matter regions were removed from the data through linear regression [**?**]. Then, the fMRI data were parcellated into 90 regions using an automated anatomical labeling template [**?**]. For each subject, the mean time series of each region was obtained by simply averaging the time series of all voxels within that region.

2.5 Brain network construction

To measure the functional connectivity among regions, we calculated the Pearson correlation coefficients between any possible pair of regional time series, and then obtained a temporal correlation matrix (90x90) for each subject. We applied Fisher's r-to-z transformation to improve the normality of the correlation matrix. Then, two-tailed one-sample t-tests were performed for all the possible 4005 i.e., $(90x89)/2$ pairwise correlations across subjects to examine whether each inter-regional correlation significantly differed from zero [**?**]. A Bonferroni-corrected significance level of P¡0.001 was further used to threshold the correlation matrix into an adjacency matrix whose element was 1 if there was significant correlation between the two brain regions and 0 otherwise. Finally, an undirected binary graph was acquired in which nodes represent brain regions and edges represent links between regions. The study of the connectivity distribution of the resulting adjacency matrix is provided in the Apendix 5.

2.6 Graph theoric analysis

Until the recent advent of graph theoretic methods in RS-fMRI, the focus was put on the identification of anatomically separated regions that show a high level of functional correlation during rest. Graph theory provides a theoretical framework to investigate the overall architecture of the brain. Thus, the emphasis has shifted from the identification of local subnetworks -default mode network, primary sensory motor network etc.- to the assessment of the topological and informational characteristics of a brain-scale complex network. The tools we use to model a system may also convey an ontological version of it, that is to say, the system under study is seen through the lens of a specific approach that necessarily shapes the observability domain. Thus, the identification of different subnetworks during rest can be seen as a by-product of the techniques used, for example identification component analysis (ICA) or clustering. Graph theory-based approaches model the brain as a complex network in which nodes represent brain regions of interest and the edges connect-

ing nodes represent relationship between nodes e.g., functional connectivity. The graph-based network provides a geometric representation to visualize brain connectivity patterns and an analytic toolbox to quantitatively characterize the overall topological organzation. Graph-based techniques have proliferated in the last years providing new insights into the structure funtion relantionship in the healthy brain, and in aging and neuropathological disorders. Prove of the utility of this approach is that notable proponents of a modularist vision of brain connectivity to understand cognition, such as Gazzaniga [20] (see [19] for an early critic of the modularist approach and anticipating a shift toward a networks) has now embraced the complex brain networks approach to understand the interplay beween structure and function in brain systems [1].

A critical aspect is to understand network robustness, that is, functional network invariance under perturbation. In essence, robustness measures the capacity of the network to perform the same function before and after a perturbation. Perturbations are events, internal or external, that elicit a change in the network configuration, as for example in, to obliterate a node or a change in the connectivity between nodes. Thus, for a given network $G(V,E)$ with an adjacency matrix A, a perturbation δ that transforms A into a new adjacency matrix A' by deleting a set of nodes W from V. Thus, the initial graph $G(V,E)$ is transformed into a new post perturbation graph $G(V-W,E-E(W))$, where $E-E(W)$ is the set of edges that do not connect any of the deleted nodes in W We want to measure the network vulnerability, to do so we calculate the geodesic path distance between any two nodes in the graph.

The network efficiency is calculated using the Latora and Marchiori network efficiency measure [25]. According to 1 a network is considered to be more efficient if the distances between pairs of nodes are smaller.The efficiency of the graph $G(V,E)$, $\Gamma(G(V,E))$ is

$$\Gamma(G) = \frac{1}{n(n-1)\sum_{i\neq j\in V}\frac{1}{d_{ij}}} \tag{1}$$

where n is the number of nodes or $|V|$ and dij is the shortest path length (the geodesic distance) between nodes i and j. Note that $0 \leq d_{ij} = d_{ji} \leq 1$.

We study network robustness based on the new network efficiency/performance measure 1 in order to investigate the network functionality when a set of nodes are obliterated. The efficiency $\Gamma(G)$ is a network centrality measure that quantifies how likely the network is robust to the deletion of nodes i.e., the network's reliability in transmitting information once a node is removed from the network. The global network efficiency is 0.3795 for young subjects and X for elder sujects. EXPLAIN

We can, furthermore, calculate the ranking of vulnerability of each node. The vulnerability of node i, $vul(i)$ represents how the deletion of the node i affects the global efficiency of the resulting network and is given by the expression:

$$Vul(i) = \frac{\Gamma(G(V,E)) - \Gamma(G(V-i,E))}{\Gamma}(G(V,E)) \tag{2}$$

In Table **??** is shown the vulnerability value for each of the AAL regions and their Broadmann area. Interestingly, there are some nodes that when removed, the overall

network vulnerability decreased -nodes 89 to 57 for young subjects and nodes Y to Z in the table. In young subjects, the deletion of node 89 results in an increase in the overall network efficiency of a 22.7% according to formula 2. The network vulnerability deteriorates for the the remaining 63 nodes. The worst performance occurred when nodes 60, 31, 50, 46, 73 and 30 are deleted in which case vulnerability of the ovrall resulting netwoirk is increased between 20% and 10%. In the case of elder individuals, COMPLETE. RELATE RESULTS with the litterature on RSNs . What can we say about this vulnerability ranking and the robustness of RSNs and the NDH

2.7 Information theoric analysis on Markov chains

The undirected binary graph depicted in figure **??** is the geometric characterisation of the adjacency matrix A, in which $a_{ij} = 1$ if AAL region i and AAL region j show a significant correlation and $a_{ij} = 0$ otherwise. We transform the binary adjacency matrix A into a weighted adjacency matrix T where $T_{ij} = \frac{a_{ij}}{\sum_j a_{ij}}$. The new graph has the same number of nodes each with a weight $T_{ij} \geq 0$ on the link that connects node i and node j. $T_{ij} = 0$ if nodes are not connected and symmetry $T_{ij} = T_{ji}$ is also preserved. Now, let us consider a random walk -a particle moves from node to node- on the weighted undirected graph T. Thus, a random walk $X_n X_n \in \{1,2,\ldots n\}$ is a list of nodes visited by the particle. The probability that the particle moves from i to j is given by T_{ij}. This stochastic process defines a Markov chain because the probability that that the particle moves from state n to state n+1 is independent of the previous states, that is, $P(X_{n+1} = x_{n+1}|X_n = x_n) = P(X_{n+1} = x_{n+1}|X_n = x_n, X_{n-1} = x_{n-1}, \ldots, X_1 = x_1) \forall x_1, \ldots, x_n \in \mathscr{X}$. The stationary distribution of the random walk on the undirected graph is $\mu = \frac{k_i}{2E}$, where k_i is the connectivity degree of node i and E is the total number of links contained in the graph. Thus, the stationary distribution is given by the 90 dimensional vector $\mu = \{\frac{k_1}{2E}, \frac{k_2}{2E}, \ldots, \frac{k_n}{2E}$. It ought to be noted that the stationary distribution does not depend on the number of nodes, but only on the total number of links E, and the weight of the neighbor nodes. Thus, the stationary distribution holds the local property that it is not altered by changes in the weights of non neighbors nodes, while keeping the total weight of the graph constant. The entropy rate of a stochastic prcess represents the rate at which the entropy of a sequence e.g., a random walk, grow with n. Formally, for the stochastic process $\mathscr{X} = \{X_1, \ldots, X_i, \ldots, X_n\}$ the entropy rate is given by

$$H(\mathscr{X}) = \lim_{n \to \text{inf}} \frac{1}{n} H(X_1, X_2, \ldots, X_n) \tag{3}$$

For a stationary Markov chain, the entropy rate is

$$H(\mathscr{X}) = \lim_{n \to \text{inf}} H(X_n|\, X_{n-1}, \ldots, X_1) = \lim_{n \to \text{inf}} H(X_n|X_{n-1}) = \lim_{n \to \text{inf}} H(X_2|X_1) \tag{4}$$

The entropy rate is computed with the stationary distribution of the Markov chain μ and the transition matrix T. Then

$$H(\mathscr{X}) = -\sum_{ij} \mu_i T_{ij} \log T_{ij} \tag{5}$$

We define a Markov processes for both the young subjects and the elder ones with their transition matrix given by T^y_{ij} and T^e_{ij} respectively

$$T^y_{ij} = \frac{A^y_{ij}}{\sum_j A^y_{ij}}, T^e_{ij} = \frac{A^e_{ij}}{\sum_j A^e_{ij}} \tag{6}$$

where A^y_{ij} and A^e_{ij} are the binary adjacency matrix of the young and the elder subjects. Thus, the entropy rate is

$$\begin{aligned} H(X^y) &= -\sum_{ij} \mu^y_i T^y_{ij} \log T^y_{ij} \\ H(X^e) &= -\sum_{ij} \mu^e_i T^e_{ij} \log T^e_{ij} \end{aligned} \tag{7}$$

where $T^y_{ij} = \frac{A^y_{ij}}{\sum_j A^y_{ij}}$ and $T^e_{ij} = \frac{A^e_{ij}}{\sum_j A^e_{ij}}$

We calculate the entropy rate for the resulting markov process after having delete a node or a group of nodes in both young and elder subjects. Thus, the relative entropy of the stochastic process defined by the set of states $\mathscr{X}' = \mathscr{X} - X_k$ in which the set of nodes X_k and their respective edges has been removed from the initial chain $\mathscr{X}$, is

$$H(X') = -\sum_{ij, i,j \not\subset k} \mu_i T_{ij} \log T_{ij} \tag{8}$$

3 Results

We have analyzed the functional connectivity in resting state of both young and elder individuals. The nodes representing the ninety brain regions based on the AAL parcelation have been ranked in terms of their impact in terms of network robustness upon removal. Interestingly we find that in both elder and young groups the removal of certain nodes does not necessarily triggers a decrease in network robustness, the obliteration of certain nodes may also produces a positive impact in the network function, increasing the network robustness when the node is removed.

The results show that in young subjects, that the nodes with a positive impact are ... compared with elder subjects ...

In the second part we use information-theoretic measures to study the impact of the removal of nodes in the network. First, we model the network flows in terms of a stationay Markov chain which describes how a particle walks randomly from node

to node, in both the young and elder functional connectivity graph. The probability transition matrix is derived from the binary adjacency matrix using the local property of connectivity degree. The entropy rate of a random walk on a graph in which a node or grop of nodes has been removed is calcultated.

The results show that in young subjects, after he removal of the nodes with a positive impact the entropy rate is ¿ ¡? than in the case of elder subjects.

4 Discussion

However, it might be emphasized that the empirical validation of the network degeneration hypothesis does not tell us much about the mechanisms that mediate in the alleged network connectivity sensitivity to neuropathological syndromes.

4.1 A Theory of Robustness

Standard approaches to network robustness aere based on the different beween informational flow pre and post a network injury. for example, as is shown in section **??** the impact of the removal of a network node together with its links is calculated by substacting the global efficiency of the original network to the efficiency of the injured network. An alternative approach to robustness is assuming that the information flow in the graph can be modeled a stationary Markov process. We can then define robustness of node n and of the average robustness of the network relative to the removal of a node or group of nodes. Note that in this approach robustness is always relative to a particular injury e.g., the deletion of node rather than a generic property

4.2 Relative entropy

Markov chains assumes that knowing the present state, the future of the system is independent of the past, that is, the present state contains all the information about the past states. The relative entropy $D(p||q)$ for two probability distribution p and q on the state space of a Markov chain $\mathscr{X}$ is

$$D(p||q) = \sum_{x \in \mathscr{X}} p(x) \log \frac{p(x)}{q(x)} \tag{9}$$

The relative entropy is also known as Information divergence and Kullback-Leibier distance. This divergence (it is not a truly distance because is not symmetric i.e., $D(p||q) \neq D(p||q)$) is always positive or equal to zero when both probability distri-

butions are equal. Mutual information is a particular case of the relative entropy D which arises as the exponent in the probability of error in a hypothesis test between two distributions (2^{-nD}). It is a natural measure of distance between distributions. The relative entropy D is a measure of the inefficiency of assuming that the distribution is q when the true distribution is p or the expected difference in the number of bits required to code samples from probability distribution q when using a code based on probability distribution q.

We are interested in quntify the effect of the obliteration of different nodes with ther vulnerability index associated as described in section **??**. thus, we calculate the information divergence, relative entropy, or Kullback-Leibler (KL) distance of a transformation T_a (post node removal) from a transformation T_b (pre node removal) with respect to an input distribution μ

Therefore, we define the robustness against the exclusion of Y as the information flow Y ! Z minus the exclusion dependence. This leads to the following formula:

This measures the amount of statistical dependence between x and y that is used for computing z in order to compensate the exclusion of y. The robustness vanishes if for all x and all z

4.3 KL

Contrary to standard robustness studies reviewed in section **??** that measure the effect of network insults -typically node removal- in terms of macroscopic properties such as cost, efficiency or entropy, here we focus on the different adaptive processes that may follow the network disruption, and we are able to identify the strategies that promote function invariance. The Kullback-Leibler distance allows to answer the question of which of a set of approximating models is closest to the original model f. This is a classical problem of model selection in which the Kullback-Leibler distance allows elucidate which model in a set of candidate models, $g(x|\theta)$, is the closest to the true model $f(x)$. Accordingly, the best candidate is that with minimum distance. Thus, the minimum distance between f and g in the case of discrete distributions is given by:

$$KL(f,g) = \sum_{i=1}^{n} p_i \log(\frac{p_i}{q_i}) \tag{10}$$

where n is the number of possible outcomes of the underlying random variable, p_i is the probability distribution of the ith outcome and q_i is the approximating probability distribution. The KL distance is not a true metric since is not symmetric, as the distance is different from the distance. For a more in detailed description of KL, see [11]

It is important to note that KL cannot be computed unless we have a full knowledge of both the true model f and the parameters θ in g_θ. While this requirement is often unrealistic for observational studies, specially in biology, it holds in the present case [**?**]. The applicability of this approach relies upon the fact that "true

model" f is given by the network adjacency matrix T prior to the insult d_A and the parameters θ in g_θ can be assigned to a vector $b_i = b_{i1}, \ldots, b_{i|A|}$ that assigns specific weights to each node in T_A, the resulting adjacency matrix of the perturbation d_A readjusted with a bias or strategy b_i, in which the passage through certain nodes are favored related to others. For example, a bias or adaptive strategy in which random walkers are more likely to visit nodes with highest betweenness centrality can be constructed straight forward by increasing the weight of the edges that lead to those nodes.

4.4 Misc

Traditionally, in task-related studies the resting state is assumed to be the baseline or control state with no functional significance. Recent advances in fMRI techniques have drastically challenged this view and have showed that "the baseline state of the brain is by no means an inactive state" (Damoiseaux, 2006). These slow fluctuations in BOLD signal found in resting subjects, are highly coherent within either structural or functional networks in the human brain. Therefore, exploring these fluctuations could lead to a better understanding of the brain's intrinsic or spontaneous neural activity. How these network properties are modified during normal development, aging or pathological conditions is still under debate. For example, it is unclear whether Alzheimer's disease affects local or global connectivity, or if connectivity is attenuated as in the Default Mode Network (DMN) (Greicius et al., 2004) or on the contrary, Alzheimer's disease may induce an increase in functional connectivity that compensates for the disease related atrophy of affected regions (Sanz-Arigita,2010).

RS- fMRI have been successfully used in classification of subjects with AD and MCI versus healthy controls. Connectivity changes in the default mode network can be used as markers of pathological conditions. For example, patients with tivity in the salience network. Alzheimer disease demonstrated decreased connectivity in the default mode network but increased connectivity in the salience network. Other studies rather than focusing on specific RSNs -default mode network- investigate altered connectivity patterns at a brain-wide level. The hypothesis that neurological disorders target large-scale functional and structural networks [40] rather than specific loci or sub-networks, calls for an integrative network-based approach.

Schizophrenia patients show a decreased functional connectivity during rest [27] suggesting a suboptimal information integration between regions of the brain network [35] AD patients show clustering coefficients significantly lower in patients compared with controls. There is a growing body of evidence that neurodegenerative disease targets specific large-scale brain networks, and clinical applications. Altered resting-state functional connectivity patterns have been shown in an impressive range of pathologies and conditions - Alzheimer's disease, schizophrenia, multiple sclerosis, Parkinson's disease, depression, autism, and even attention deficit/ hyper-

activity disorder. See [26] for a review on clinical applications of rs-fMRI at the single subject level.

Despite the variability in the data acquisition protocols, statistical data analysis and gropus of subjects employed by different researchers, the litterature consistenly shows an overlap of functionally linked networks in the brain during resting state. The most commonly reported resting state networks are at least eight: the primary sensorimotor network, the primary visual and extra-striate visual network, bilateral temporal/insular and anterior cingulate cortex regions, left and right lateralized networks consisting of superior parietal and superior frontal regions, and the default mode network [44].

The method that study BOLD fluctuations that spontaneously emerge during awake rest is called resting state fMRI (R-fMRI), and the networks that are identified with such a methodology are resting state networks (RSNs). Resting state networks have been identified in a panoply of imaging techniques including fMRI [4], PET [36] (first identification of the Default Mode Network), near-infrared spectroscopy (NIRS) [39], EEG [32], [6] and fMRI combined with diffusion-based studies -diffusion tensor imaging (DTI) [45] and high angular resolution diffusion imaging (HARDI) [31]. Data analysis of resting state data falls into two gropus: seed-based and model-free methods. In the former, a functional connectivity map of regions of interest or seeds is obtained. The map represents the correlation between the resting-state time-series of the different seeds, which have been a priori selected [10], [16], [8], [5]. Model-free methods also provide a connectivity map across brain regions, but here the regions of interest are obtained through statistical analysis, rather than defined a priori as in the mode-based approach. A number of model-free computational tools exist to analyse resting-state time series, including independent component analysis [3] , [13], , clustering [42], [43] and machine learning techniques such as support vector machines [30], [50]. For a critique on the use of the "minimal assumption" adopted in model-free approaches such as ICA in neuroimage data analysis, see [18].

Seed-based methods are relatively straight forward to use and conteptually simple. A disadventage is that the functional connectivity map here obtained is strictely dependent on the regions of interest previosly selected, overlooking the rest of brain areas and therefore falling to notice potentially relevant functional connection patterns. Model-free methods, on the other hand, explore functional connectivity at whole-brain scale. Independent component analysis allows direct comparison between subject groups [9], but presents the disadventage that it provides a number of different networks (components) whose biological relevance and consistency with previous findings need to be validated by other means. Note that model-based approaches avoid this dificulty by adopting the seeds or regions of interest a priori, either by selecting the relevant regions from a separate fMRI in a task experiment, or using a brain atlas in rest activity studies [47], [14].

Clustering and machine learning methods e.g., SVM, allow individual-based classification analysis. This is an important advantage to traditional group analyses of variance, and may bring important insights into disease onset prediction on individual subject basis [48]. Importantly, the above described approaches taken to-

gether show consistency in their results, that is, the functional maps tend to overlap across resting-state studies in the human brain [44].

It is important to realize that resting state networks are not the same as intrinsic connectivity networks (ICNs), which refer to network or components identified through multivariate decomposition statistical analysis e.g., independent component analysis (ICA), that show synchronous fluctuations during task performance. Therefore, RSNs are a sub class of ICNs which comprehend a set of large-scale functionally connected brain networks not only in resting state but also in task-based neuroimaging data.

References

1. Danielle S Bassett and Michael S Gazzaniga. Understanding complexity in the human brain. *Trends in cognitive sciences*, 15(5):200–209, May 2011. PMID: 21497128.
2. Danielle Smith Bassett and Ed Bullmore. Small-world brain networks. *The Neuroscientist*, 12(6):512–523, December 2006.
3. Christian F Beckmann, Marilena DeLuca, Joseph T Devlin, and Stephen M Smith. Investigations into resting-state connectivity using independent component analysis. *Philosophical transactions of the Royal Society of London. Series B, Biological sciences*, 360(1457):1001–1013, May 2005. PMID: 16087444.
4. B Biswal, F Z Yetkin, V M Haughton, and J S Hyde. Functional connectivity in the motor cortex of resting human brain using echo-planar MRI. *Magnetic resonance in medicine: official journal of the Society of Magnetic Resonance in Medicine / Society of Magnetic Resonance in Medicine*, 34(4):537–541, October 1995. PMID: 8524021.
5. Robyn Bluhm, Peter Williamson, Ruth Lanius, Jean Théberge, Maria Densmore, Robert Bartha, Richard Neufeld, and Elizabeth Osuch. Resting state default-mode network connectivity in early depression using a seed region-of-interest analysis: Decreased connectivity with caudate nucleus. *Psychiatry and Clinical Neurosciences*, 63(6):754â761, 2009.
6. Maria Boersma, Dirk J A Smit, Henrica M A de Bie, G Caroline M Van Baal, Dorret I Boomsma, Eco J C de Geus, Henriette A Delemarre-van de Waal, and Cornelis J Stam. Network analysis of resting state EEG in the developing young brain: structure comes with maturation. *Human brain mapping*, 32(3):413–425, March 2011. PMID: 20589941.
7. Randy L Buckner, Jorge Sepulcre, Tanveer Talukdar, Fenna M Krienen, Hesheng Liu, Trey Hedden, Jessica R Andrews-Hanna, Reisa A Sperling, and Keith A Johnson. Cortical hubs revealed by intrinsic functional connectivity: mapping, assessment of stability, and relation to alzheimer's disease. *The Journal of neuroscience: the official journal of the Society for Neuroscience*, 29(6):1860–1873, February 2009. PMID: 19211893.
8. Randy L Buckner and Justin L Vincent. Unrest at rest: default activity and spontaneous network correlations. *NeuroImage*, 37(4):1091–1096; discussion 1097–1099, October 2007. PMID: 17368915.
9. Sharon Chen, Thomas J. Ross, Wang Zhan, Carol S. Myers, Keh-Shih Chuang, Stephen J. Heishman, Elliot A. Stein, and Yihong Yang. Group independent component analysis reveals consistent resting-state networks across multiple sessions. *Brain research*, 1239:141–151, November 2008. PMID: 18789314 PMCID: PMC2784277.
10. D Cordes, V M Haughton, K Arfanakis, G J Wendt, P A Turski, C H Moritz, M A Quigley, and M E Meyerand. Mapping functionally related regions of brain with functional connectivity MR imaging. *AJNR. American journal of neuroradiology*, 21(9):1636–1644, October 2000. PMID: 11039342.
11. Thomas M. Cover and Joy A. Thomas. *Elements of Information Theory*. Wiley-Interscience, August 1991.

12. J S Damoiseaux, S A R B Rombouts, F Barkhof, P Scheltens, C J Stam, S M Smith, and C F Beckmann. Consistent resting-state networks across healthy subjects. *Proceedings of the National Academy of Sciences of the United States of America*, 103(37):13848–13853, September 2006. PMID: 16945915.
13. M De Luca, C F Beckmann, N De Stefano, P M Matthews, and S M Smith. fMRI resting state networks define distinct modes of long-distance interactions in the human brain. *NeuroImage*, 29(4):1359–1367, February 2006. PMID: 16260155.
14. Andreia V Faria, Suresh E Joel, Yajing Zhang, Kenichi Oishi, Peter C M van Zjil, Michael I Miller, James J Pekar, and Susumu Mori. Atlas-based analysis of resting-state functional connectivity: evaluation for reproducibility and multi-modal anatomy-function correlation studies. *NeuroImage*, 61(3):613–621, July 2012. PMID: 22498656.
15. Michael D Fox, Maurizio Corbetta, Abraham Z Snyder, Justin L Vincent, and Marcus E Raichle. Spontaneous neuronal activity distinguishes human dorsal and ventral attention systems. *Proceedings of the National Academy of Sciences of the United States of America*, 103(26):10046–10051, June 2006. PMID: 16788060.
16. Peter Fransson. Spontaneous low-frequency BOLD signal fluctuations: an fMRI investigation of the resting-state default mode of brain function hypothesis. *Human brain mapping*, 26(1):15–29, September 2005. PMID: 15852468.
17. Peter Fransson. How default is the default mode of brain function?: Further evidence from intrinsic BOLD signal fluctuations. *Neuropsychologia*, 44(14):2836–2845, 2006.
18. Karl J Friston. Modes or models: a critique on independent component analysis for fMRI. *Trends in Cognitive Sciences*, 2(10):373–375, October 1998.
19. J.M. Fuster. The module: crisis of a paradigm book review, "the new cognitive neurosciences" 2nd edition, m.s. gazzaniga, editor-in-chief, mit press. *Neuron*, (26):51–53, 2000.
20. Michael S. Gazzaniga, editor. *The New Cognitive Neurosciences: Second Edition*. The MIT Press, 2 edition, November 1999.
21. Michelle Hampson, Bradley S Peterson, Pawel Skudlarski, James C Gatenby, and John C Gore. Detection of functional connectivity using temporal correlations in MR images. *Human brain mapping*, 15(4):247–262, April 2002. PMID: 11835612.
22. M D Hunter, S B Eickhoff, T W R Miller, T F D Farrow, I D Wilkinson, and P W R Woodruff. Neural activity in speech-sensitive auditory cortex during silence. *Proceedings of the National Academy of Sciences of the United States of America*, 103(1):189–194, January 2006. PMID: 16371474.
23. Marcus Kaiser, Robert Martin, Peter Andras, and Malcolm P. Young. Simulation of robustness against lesions of cortical networks. *European Journal of Neuroscience*, 25(10):3185–3192, 2007.
24. Salla-Maarit Kokkonen, Juha Nikkinen, Jukka Remes, Jussi Kantola, Tuomo Starck, Marianne Haapea, Juho Tuominen, Osmo Tervonen, and Vesa Kiviniemi. Preoperative localization of the sensorimotor area using independent component analysis of resting-state fMRI. *Magnetic resonance imaging*, 27(6):733–740, July 2009. PMID: 19110394.
25. Vito Latora and Massimo Marchiori. Efficient behavior of small-world networks. *Physical Review Letters*, 87(19):198701, October 2001.
26. M H Lee, C D Smyser, and J S Shimony. Resting-state fMRI: a review of methods and clinical applications. *AJNR. American journal of neuroradiology*, August 2012. PMID: 22936095.
27. Meng Liang, Yuan Zhou, Tianzi Jiang, Zhening Liu, Lixia Tian, Haihong Liu, and Yihui Hao. Widespread functional disconnectivity in schizophrenia with resting-state functional magnetic resonance imaging. *Neuroreport*, 17(2):209–213, February 2006. PMID: 16407773.
28. Wei Liao, Zhiqiang Zhang, Zhengyong Pan, Dante Mantini, Jurong Ding, Xujun Duan, Cheng Luo, Guangming Lu, and Huafu Chen. Altered functional connectivity and small-world in mesial temporal lobe epilepsy. *PLoS ONE*, 5(1):e8525, January 2010.
29. Yong Liu, Meng Liang, Yuan Zhou, Yong He, Yihui Hao, Ming Song, Chunshui Yu, Haihong Liu, Zhening Liu, and Tianzi Jiang. Disrupted small-world networks in schizophrenia. *Brain: a journal of neurology*, 131(Pt 4):945–961, April 2008. PMID: 18299296.

30. Anton Lord, Dorothea Horn, Michael Breakspear, and Martin Walter. Changes in community structure of resting state functional connectivity in unipolar depression. *PLoS ONE*, 7(8):e41282, August 2012.
31. Mark J Lowe, Erik B Beall, Ken E Sakaie, Katherine A Koenig, Lael Stone, Ruth Ann Marrie, and Micheal D Phillips. Resting state sensorimotor functional connectivity in multiple sclerosis inversely correlates with transcallosal motor pathway transverse diffusivity. *Human brain mapping*, 29(7):818–827, July 2008. PMID: 18438889.
32. D. Mantini, M. G. Perrucci, C. Del Gratta, G. L. Romani, and M. Corbetta. Electrophysiological signatures of resting state networks in the human brain. *Proceedings of the National Academy of Sciences*, 104(32):13170–13175, August 2007.
33. Sergei Maslov and Kim Sneppen. Specificity and stability in topology of protein networks. *arXiv:cond-mat/0205380*, May 2002. Science, 296, 910-913 (2002).
34. Marsel Mesulam. Defining neurocognitive networks in the BOLD new world of computed connectivity. *Neuron*, 62(1):1–3, April 2009. PMID: 19376059.
35. Sifis Micheloyannis, Ellie Pachou, Cornelis Jan Stam, Michael Breakspear, Panagiotis Bitsios, Michael Vourkas, Sophia Erimaki, and Michael Zervakis. Small-world networks and disturbed functional connectivity in schizophrenia. *Schizophrenia research*, 87(1-3):60–66, October 2006. PMID: 16875801.
36. M E Raichle, A M MacLeod, A Z Snyder, W J Powers, D A Gusnard, and G L Shulman. A default mode of brain function. *Proceedings of the National Academy of Sciences of the United States of America*, 98(2):676–682, January 2001. PMID: 11209064.
37. Marcus E. Raichle and Debra A. Gusnard. Intrinsic brain activity sets the stage for expression of motivated behavior. *The Journal of Comparative Neurology*, 493(1):167–176, 2005.
38. Ernesto J Sanz-Arigita, Menno M Schoonheim, Jessica S Damoiseaux, Serge A R B Rombouts, Erik Maris, Frederik Barkhof, Philip Scheltens, and Cornelis J Stam. Loss of 'small-world' networks in alzheimer's disease: graph analysis of FMRI resting-state functional connectivity. *PloS One*, 5(11):e13788, 2010. PMID: 21072180.
39. Shuntaro Sasai, Fumitaka Homae, Hama Watanabe, Akihiro T Sasaki, Hiroki C Tanabe, Norihiro Sadato, and Gentaro Taga. A NIRS-fMRI study of resting state network. *NeuroImage*, 63(1):179–193, October 2012. PMID: 22713670.
40. William W Seeley, Richard K Crawford, Juan Zhou, Bruce L Miller, and Michael D Greicius. Neurodegenerative diseases target large-scale human brain networks. *Neuron*, 62(1):42–52, April 2009. PMID: 19376066.
41. Kaustubh Supekar, Vinod Menon, Daniel Rubin, Mark Musen, and Michael D. Greicius. Network analysis of intrinsic functional brain connectivity in alzheimer's disease. *PLoS Computational Biology*, 4(6), June 2008. PMID: 18584043 PMCID: PMC2435273.
42. Bertrand Thirion, Silke Dodel, and Jean-Baptiste Poline. Detection of signal synchronizations in resting-state fMRI datasets. *NeuroImage*, 29(1):321–327, January 2006. PMID: 16129624.
43. Martijn van den Heuvel, Rene Mandl, and Hilleke Hulshoff Pol. Normalized cut group clustering of resting-state fMRI data. *PLoS ONE*, 3(4):e2001, April 2008.
44. Martijn P van den Heuvel and Hilleke E Hulshoff Pol. Exploring the brain network: a review on resting-state fMRI functional connectivity. *European neuropsychopharmacology: the journal of the European College of Neuropsychopharmacology*, 20(8):519–534, August 2010. PMID: 20471808.
45. Martijn P van den Heuvel, RenÃ© C W Mandl, RenÃ© S Kahn, and Hilleke E Hulshoff Pol. Functionally linked resting-state networks reflect the underlying structural connectivity architecture of the human brain. *Human brain mapping*, 30(10):3127–3141, October 2009. PMID: 19235882.
46. Justin L Vincent, Itamar Kahn, Abraham Z Snyder, Marcus E Raichle, and Randy L Buckner. Evidence for a frontoparietal control system revealed by intrinsic functional connectivity. *Journal of neurophysiology*, 100(6):3328–3342, December 2008. PMID: 18799601.
47. Jinhui Wang, Liang Wang, Yufeng Zang, Hong Yang, Hehan Tang, Qiyong Gong, Zhang Chen, Chaozhe Zhu, and Yong He. Parcellation-dependent small-world brain functional networks: a resting-state fMRI study. *Human brain mapping*, 30(5):1511–1523, May 2009. PMID: 18649353.

48. Ying Wang, Yong Fan, Priyanka Bhatt, and Christos Davatzikos. High-dimensional pattern regression using machine learning: from medical images to continuous clinical variables. *NeuroImage*, 50(4):1519–1535, May 2010. PMID: 20056158.
49. Strogatz S.H. Watts D.J. Collective dynamics of 'small-world' networks. *Nature*, 393:2440442, 1998.
50. Ling-Li Zeng, Hui Shen, Li Liu, Lubin Wang, Baojuan Li, Peng Fang, Zongtan Zhou, Yaming Li, and Dewen Hu. Identifying major depression using whole-brain functional connectivity: a multivariate pattern analysis. *Brain*, March 2012.

5 Appendix

From our analysis we exclude the possibility that the connectivity distribution follows a power law. The log-log plot of the nodes connectivity cumulative probability distribution (Figure 1) is a nonoptimal fit with a straight line (solid line)). The next step is to study whether the connectivity network is scale free or a small world network. Note that in small world networks degree distributions other than power law are possible. For example, a power law can be cut-off by a Gaussian or exponential distribution, which apparently is the above scenario for the tail (Figure1). However, the figure 1 shows that only in the middle of the distribution we may have something similar to a power law. The extremes show an exponential or Gaussian kind of signature. The figure 2 depicts a good fit between with a normal distribution but only for connectity values between 5 to 15.

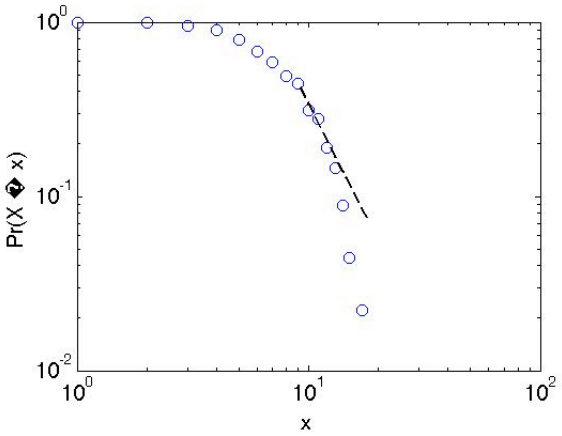

Fig. 1 Caption

In order to asses the network topology of the network depicted in Figure 3we need first to determine the randomized counterpart of the given network in order to relate the graph properties of the original network with those of the randomly

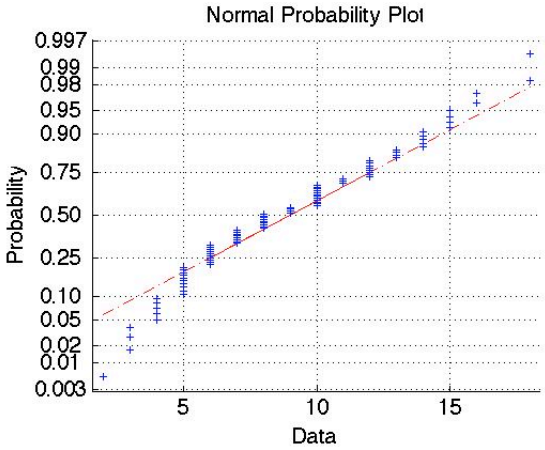

Fig. 2 Caption

built synthetic networks. Thus, the randomly built synthetic networks provide the null model that we need in order to identify whether the graph invariants in the real network are over represented or under represented in relation with the synthetic networks.

Here we explain how the generate a pool of randomly generated random network, then we compare the metric for the real network with this pool. There are a number of different algorithms that may generate a pool of random network that maintain specific characteristics (graph invariants) that we wish the random network hold, such as connectivity degree, number of nodes, number of edges etc. First, we use the Renyi-Erdos model to provide a population of random networks with the same number of nodes and edges than the brain network (See Appendix for details). We obtain the global path length $\lambda = \frac{\lambda_{real}}{\lambda_{random}} = \frac{0.0881}{0.0993} = 0.8881$ and the local clustering coefficient is $\gamma = \frac{\gamma_{real}}{\gamma_{random}} = \frac{0.7790}{0.1005} = 7.7527$. Thus, $\sigma = \frac{\gamma}{\lambda} = 8.7299$, which indicates that the clustering tin the real network is much higher than in the counterpart random networks and the distance in the characteristic path length between the real and the randomly generated network is close to 1. A different alternative to create random networks is using the Maslov's algorithm [33]. Here the degree of the nodes is preserved, that is, each node in the generated random network will have the same number of immediate neighbors. In the left side of Figure 4is shown the systematic deviations of the ratio $P(K0,K1)/P(K0,K1))$ from 1, and on the right side is depicted the statistical significance of the deviations. Both plots combined reveals regions on the plane were connections between brain regions are significantly enhanced or supressed compared to the null model. The red region in the left side plot indicates the tendency of poorly connected nodes to associate with other poorly connected nodes (less than four neighbors), blue regions in the upper left and lower right shows the reduced likelihood that highly connected nodes are

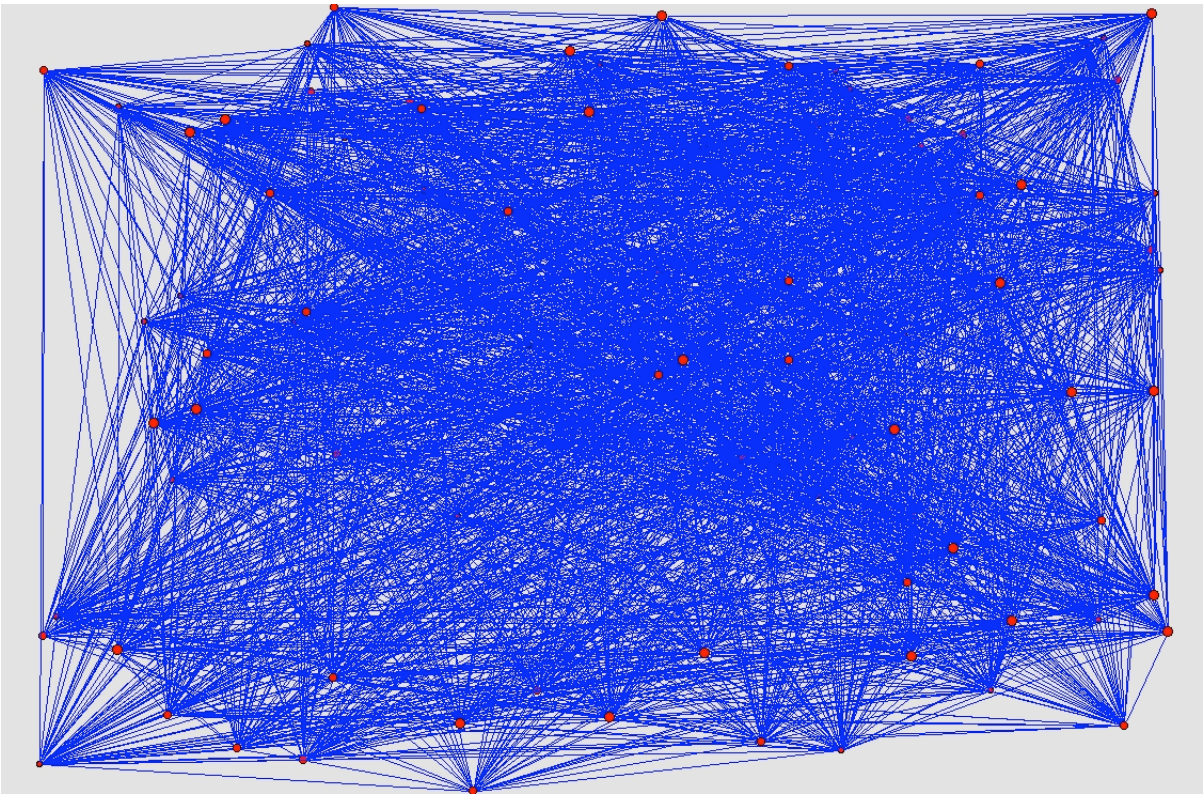

Fig. 3 Caption Pajek

directly linked with poorly connected nodes and viceversa. The Z scores plot on the right of Figure 4 is the normalized statistical significance of the deviations or $Z(K0,K1) = \frac{(P(K0,K1)-P(K0,K1)}{\sigma_r(K0,K1)}$, where $\sigma_r(K0,K1)$ is the the standard deviation of $P(K0,K1)$ in 100 realizations of a randomized network.

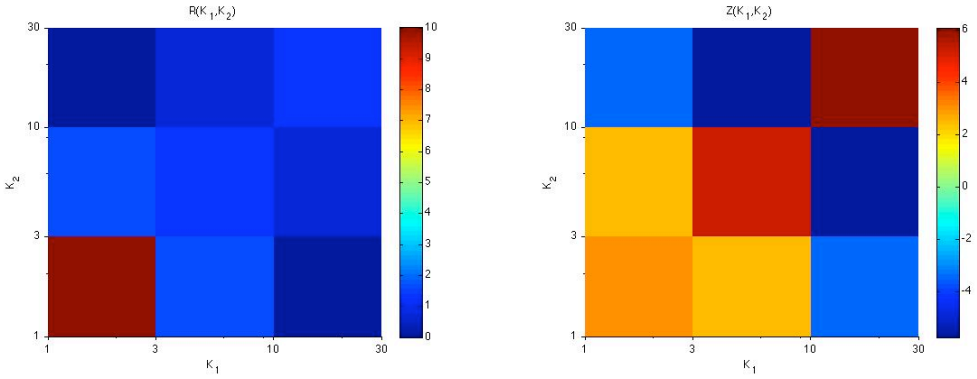

Fig. 4 Caption